

Correspondence

Time-Varying, 3-D Echocardiography Using a Fast-Rotating Probe

Jérôme Blancher, Christophe Léger, *Member, IEEE*, and Long Dang Nguyen

Abstract—A fast continuous rotating ultrasound scan-head transducer was used to perform three-dimensional (3-D) echocardiography with 2-D images acquired during a single cardiac cycle. The 3-D images were reconstructed by interpolating 2-D data acquired with the probe. Two experiments were carried out to validate the image reconstructions. A dynamic cardiac phantom was used as a known reference to compare the minimal and maximal volumes estimated manually on the reconstructed 3-D images. The left ventricle (LV) volume of 30 healthy volunteers also were estimated using a semiautomatic ellipse approach and compared to measurements obtained with standard 2-D examination. Results showed a good agreement between 3-D and reference measurements.

I. INTRODUCTION

TWO-DIMENSIONAL (2-D) echocardiography is widely used in cardiology due to its specific advantages compared to other cardiac imaging techniques. For the patients, it is noninvasive and has no known bioeffects (within the clinically used ultrasound frequency and power range). It also provides fast, ambulatory, and inexpensive examinations. However, 2-D echocardiography has limitations due to the moderate quality of ultrasound imaging and the difficulty of locating images in space accurately. Therefore, a 2-D echocardiography examination is highly dependent on the ability of the cardiologist to manipulate the ultrasound transducer and to obtain correct images of the heart. This is particularly true for volume estimations, which are conventionally carried out using a rough heart modeling fitted to 2-D data. More accurate and reliable results would be obtained with 3-D echocardiography.

During the last decade, considerable progress has been made in performing 3-D echocardiography [1]. Two main types of probes have been developed. First, ultrasound volume images are produced using adapted 2-D transducers: the sensor is able to move along parallel planes [2], to oscillate [3], [4], to rotate [5], [6], or to be moved in any direction using free-hand scanning and an accurate localization of the transducer [7]. Interesting results have been obtained with transthoracic or transesophageal 2-D probes, but all the devices based on these techniques need to be

synchronized on the electrocardiogram (ECG) to accumulate data, assuming that many consecutive heartbeats are identical. Second, a new type of probe, based on matrix array transducers, produce real time 3-D (RT3D) ultrasound scans and acquire pyramidal images [8]–[10]. However, RT3D imaging requires specific, complex, and expensive 3-D ultrasound systems, and it needs to be improved as the resolution is still lower than for 2-D probes.

In this correspondence, we present the reconstruction of a 3-D echocardiographic image set using a fast rotating ultrasound scan-head (linked to a standard 2-D ultrasound system) that acquires 2-D images within a single cardiac cycle [11], [12]. To validate the 3-D image reconstruction process, a dynamic cardiac phantom was used as a known reference to compare the minimal and maximal volumes estimated manually on the reconstructed 3-D images. A clinical study also was carried out at the Hospital Center in Orléans on 30 healthy subjects. During this trial, left ventricle (LV) volumes were estimated on 3-D images using an ellipse approach and compared with measurements obtained with a classical 2-D examination.

II. MATERIALS AND METHODS

A. System Description

A prototype of a fast rotating probe designed by Vermon (Tours, Cedex, France) and described in [12] was connected to an ATL/Philips HDI 5000 (Philips Medical Syystems, Andover, MA) ultrasound system. The transducer array rotated continuously inside the probe with a speed of eight rotations per second. The direction of the motor was inverted every two rotations due to the electrical connection between the array and the device. The rapid deceleration and acceleration during the inversion had no critical impact on the probe speed stability because the time of inversion was less than 2.5 ms and the angular speed variation of the probe did not exceed $6^\circ/\text{ms}$ at the beginning of the inversion. An optical encoder was used to measure the angular position of the sensor with 0.18° of accuracy. The probe operated at 3.5 MHz. The image frame rate was set at 128 Hz. Under typical heart beat frequency (60 beats per minute), 128 digital images (257×320) were acquired within a single cardiac cycle without ECG synchronization. An LV volume description was obtained with each half rotation (π rad) of the probe, which corresponded approximately to eight images (acquired in 1/16th of a second, that is to say, 1/16th of a 1 Hz cardiac cycle) grouped to build a single 3-D image (Figs. 1 and 2). With the probe operating at eight rotations per second, 16 3-D images can be reconstructed within 16 successive intervals of a typical heart beat, each 3-D image being reconstructed using data acquired during one interval.

Manuscript received May 26, 2003; accepted December 29, 2003.

J. Blancher and C. Léger are with the Laboratoire d'Electronique Signaux Images (LESI), Université d'Orléans, 45067 Orléans Cedex 2, France (e-mail: Christophe.Leger@univ-orleans.fr).

L. D. Nguyen is with the Service de Cardiologie, Centre Hospitalier Régional d'Orléans (CHRO), 45067 Orléans Cedex 2, France.

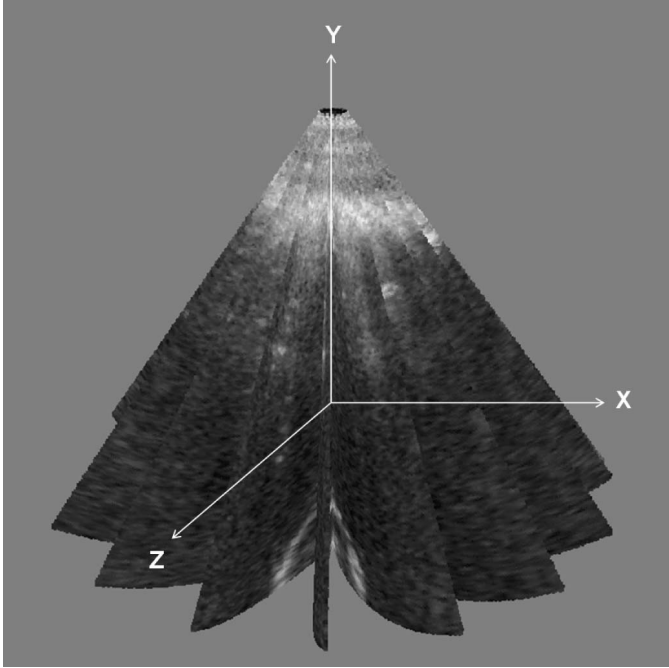


Fig. 1. Images acquired with the fast-rotating probe and positioned in a 3-D space after the 2-D to 3-D transformation.

B. 3-D Image Reconstruction

The global displacement of the ultrasound beam is composed of a classical angular movement $\alpha(t)$ and a rotation $\varphi(t)$, producing beam trajectories along conic ruled surfaces as shown on Figs. 1 and 3. The pixel coordinates $I(i, j)_{\mathbb{N}^2}$ of the planar 2-D images acquired with the ultrasound system are expressed in a 3-D space $I(x, y, z)_{\mathbb{R}^3}$ using the straightforward equation:

$$(x, y, z) = f(i, j) \Leftrightarrow \begin{cases} x = (j_p - j) \cdot \cos[\varphi(t)] \\ y = i_p - i \\ z = (j_p - j) \cdot \sin[\varphi(t)] \end{cases}, \quad (1)$$

where (i_p, j_p) are the coordinates of the probe in the 2-D images.

During the acquisition of images, the angular variation of $\varphi(t)$ is linear (between two rotations) and measured at regular time steps with the optical-coder:

$$\varphi(t) = \frac{2\pi}{T_\varphi} \cdot t + \varphi_0, \quad (2)$$

where T_φ is the probe rotation period and φ_0 is the angular position of the probe at the beginning of the image acquisition.

The variation of $\alpha(t)$ is also linear and equal to:

$$\alpha(t) = \frac{\Delta_\alpha}{T_\alpha} \cdot t + \alpha_0, \quad (3)$$

where Δ_α is the angular sector in the 2-D images as shown on Fig. 3, T_α is the duration of one frame, and α_0 is the angular position of the ultrasound beam at the beginning of the sector acquisition.

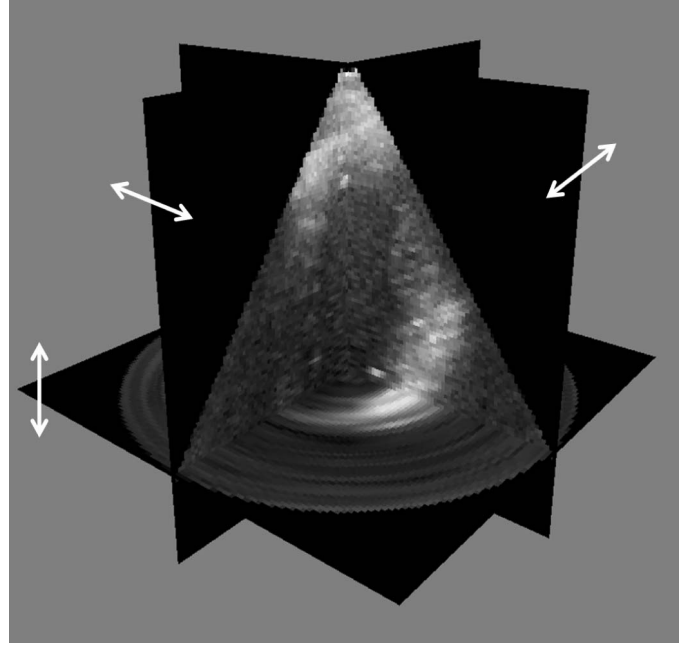


Fig. 2. Display of the 3-D echocardiographic image, after reconstruction, using three mobile planes.

For a given pixel $I(i, j)_{\mathbb{N}^2}$ of a 2-D image, $\alpha(t)$, $(-\frac{\Delta_\alpha}{2} \leq \alpha(t) \leq \frac{\Delta_\alpha}{2})$, is computed according to the relation $\arctan\left(\frac{j-j_p}{i-i_p}\right)$. Then, its value is used to calculate $\varphi(t)$, and the (x, y, z) coordinates of the pixel $I(x, y, z)_{\mathbb{R}^3}$.

Once the pixels $I(i, j)_{\mathbb{N}^2}$ have been located in the 3-D space $I(x, y, z)_{\mathbb{R}^3}$, a grey level value $\tilde{I}(i, j, k)_{\mathbb{N}^3}$ is assigned to each (i, j, k) position in the 3-D image. This is carried out with a linear interpolation between two pixels $I_0(x_0, y_0, z_0)_{\mathbb{R}^3}$ and $I_1(x_1, y_1, z_1)_{\mathbb{R}^3}$ chosen in the two images close to each (i, j, k) position.

Using this method, up to 16 3-D images ($257 \times 320 \times 320$) are computed off-line [computation time less than 5 minutes for 12 3-D images with a Pentium 4 2.0 GHz equipped with 1 Gb random access memory (RAM)]. An application has been developed to visualize the cine-loop of these time-varying, 3-D images. Specific slices of the 3-D images can be observed by moving three planes as shown on Fig. 2.

C. Phantom Validation

A 3-D gated dynamic cardiac phantom was used to validate the 3-D image reconstructions. The phantom, manufactured by the Academic Medical Center of Amsterdam and described in [14], consists of a cardiac insert fitted in a Data Spectrum (Data-Spectrum, Chapel Hill, NC) anthropomorphic torso phantom (Fig. 4). The insert is composed of two flexible silicone walls of ovoid shape, which form the endocardium and epicardium of the simulated left ventricle. A pump is used to vary the volume of the cavity smoothly to produce a realistic stroke volume curve, between diastolic and systolic volumes set here to 120 mL and 50 mL, respectively. Although the phantom is a me-

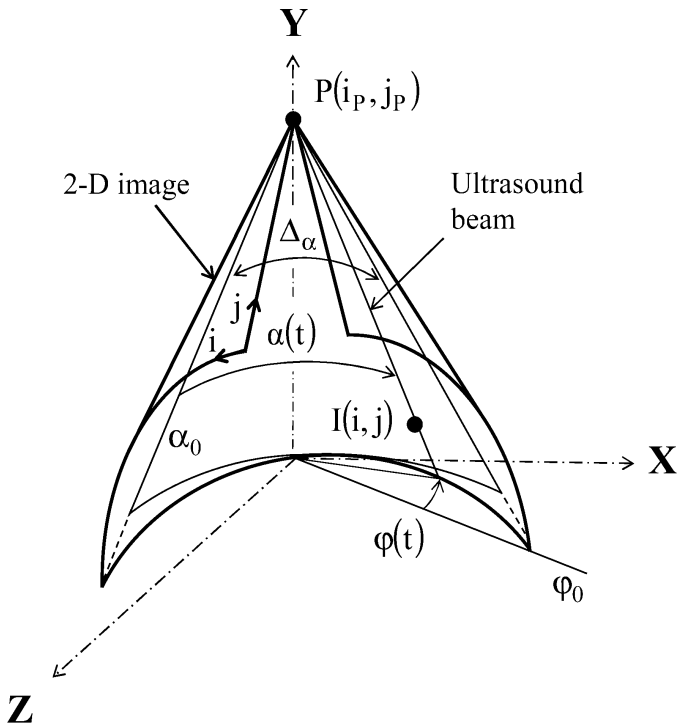


Fig. 3. Global displacement of the ultrasound beam, composed of a classical angular movement $\alpha(t)$ and a rotation $\varphi(t)$, yielding a trajectory along a conic ruled surface.

chanical device, it simulates the function of a human heart very closely. To study the inter and intra variability of the measurements, 11 acquisitions were performed using the fast rotating probe during 1 second. The described method was used to reconstruct 11 sets of 3-D images using the phantom. Within each set, two manipulators estimated end-diastolic and end-systolic volumes manually, by tracing the phantom contours on parallel cross sections of the corresponding 3-D images. Then, volume measurements were computed by summing all the traced LV areas.

D. Clinical Trial

To validate the 3-D reconstructions with data acquired under standard clinical conditions, LV volumes of healthy subjects were estimated using a fast and robust semiautomatic method. The LV volumes computed from 3-D images were compared to measurements obtained with a standard 2-D examination.

1. *Volume Estimation:* The LV volumes were estimated on 3-D images using a method based on ellipse fitting. Though many investigators have reported on techniques used to segment LV boundaries, the ellipse approach is known to be fast and robust, without requiring tedious hand tracings. In each 3-D image, the LV volume V_i was computed using the following equation:

$$V_i = \sum_{n=0}^{N-1} S_{i,n} \cdot \delta, \quad (4)$$

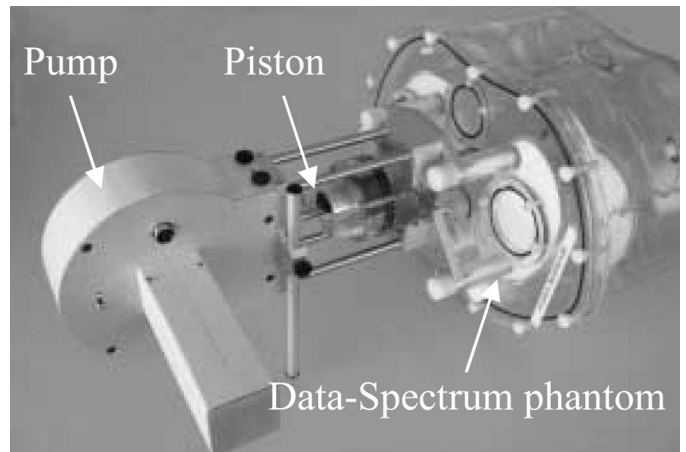


Fig. 4. Dynamic cardiac phantom, full view. Pump motor is in the foreground. In the anthropomorphic torso phantom, two imbricated membranes form the cardiac cavity.

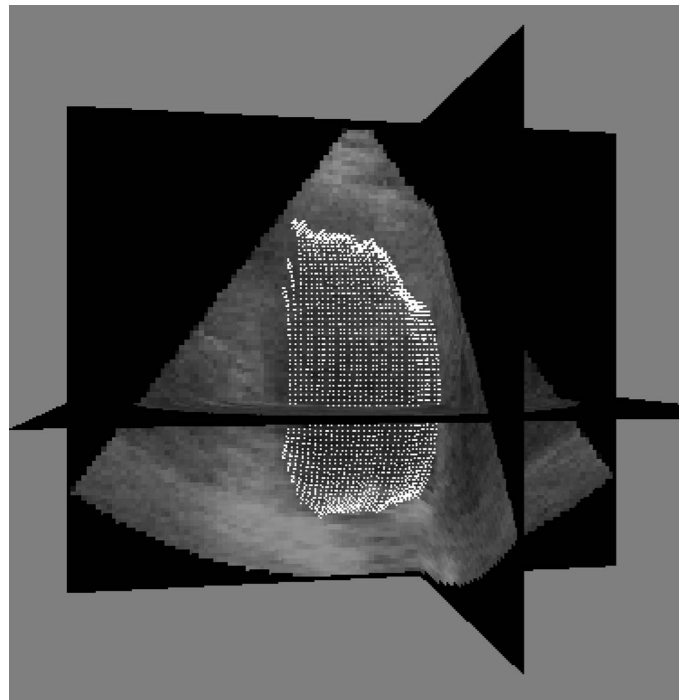


Fig. 5. Left ventricle volume estimation using ellipse fitting.

where $S_{i,n}$, $0 \leq n < N$, were the N areas of the LV within parallel cross sections of the 3-D images (Fig. 5), and δ was the distance between two consecutive parallel cross sections. Within each parallel cross section, the LV areas were approximated by the areas of ellipses fitted to LV contours (Fig. 5). The noise was reduced in the image by applying a low pass Gaussian filtering. Then, the LV contour was highlighted using thresholding. Starting from the center of the contour (assumed to be the center of the image as the LV was centered in the image, and the LV and probe axes were aligned during acquisition), ray tracing was used to extract samples of the LV contour. The ellipse parameters were computed (in less than

10 ms for each ellipse on a computer of the same type mentioned previously) from the LV contour samples according to the Fitzgibbon algorithm [13]. The ellipse areas then were measured.

2. Volume Comparison: The LV volumes estimated with the 3-D images were compared to the volumes measured during a standard 2-D examination. In the latter, the LV volume was approximated using the Simpson biplane rule, which consists in tracing manually the LV contour on a 2-D image, then approximating the volume by summing short-axis slices. Both volume estimations were processed by the same physician, but blindly in reference to each other.

Thirty healthy volunteers were recruited after informed consent. Of these, 28 were men and 2 were women; the mean age was 23 years. To be included in the test, subjects with no history of cardiac disease, including arrhythmia, were selected.

The ejection fractions (EF) and end-diastolic (V_D) and end-systolic (V_S) volumes were compared with each other using a regression analysis. Bland-Altman analysis was used to investigate the trends of differences between the two measurements.

III. RESULTS AND DISCUSSION

A. Phantom Validation

Table I presents the three measurements (respectively end-diastolic volume V_D , end-systolic volume V_S , and ejection fraction EF) estimated on 3-D images obtained from the dynamic phantom. The first column indicates the reference phantom values. The next four columns present the mean and standard deviation (SD) of measurements obtained after 11 acquisitions and reconstructions repeated by two operators. The last column represents the inter-operator variability by indicating the mean and standard deviation of the differences between the two operator measurements.

Results indicate a good agreement between volume measurements and real phantom values, for both operators. The SD of volume measurements is less than 8.3 mL for V_D (6.9% of the real V_D value), and less than 3.6 mL for V_S (7.2% of the real V_S value). The good estimation of V_D and V_S values yields an estimation of the ejection fraction from 3-D images very close to the real phantom ejection fraction (SD is less than 0.03%).

The interoperator variability study shows that the SD of the measurements difference between the two operators is less than 8.4 mL for V_D (6.9% of the real V_D value) and less than 2.1 mL for V_S (4.2% of the real V_S value) estimations. The mean of the interoperator measurements difference is about 12% of the real volumes, which is a standard value obtained in echocardiography due to the relative quality of images.

These results all indicate a good reproducibility of the measurements carried out on 3-D images, within the range of values available with the phantom.

B. Clinical Trial

Fig. 6(a) shows the LV volume estimations using the Simpson method on standard 2-D images (abscissa) versus LV volumes measured by ellipse fitting on reconstructed 3-D images (ordinates). The slope of the regression line is equal to 0.97, and the intercept is less than 5 mL. The R^2 coefficient, which evaluates the adjustment quality of data with the regression line, is equal to 0.96. Thus, volumes estimated with both methods correlate well with each other. The corresponding Bland and Altman plot presented on Fig. 6(b) indicates that, on average, volumes computed from 2-D images are underestimated by 1.53 mL compared to volumes computed from 3-D images. The SD of the differences of the two volume estimations is approximately 7.5 mL, indicating a good agreement between the two measurements. The dispersion observed for some plots is due to the ellipse approximation method, which introduces LV volume estimation errors on poorly contrasted images.

The comparison of EF computed from 2-D and 3-D images provides similar information. On Fig. 6(c), the R^2 coefficient value is equal to 0.79, indicating a high correlation between both methods for EF estimations. The R^2 coefficient value is slightly lower than the value obtained in volume comparisons. This is mainly due to the summation of the end-diastole and end-systole volume uncertainties during the EF computation. The regression line has a slope of 1.03 and intercepts at -2.1% . This near identity slope shows that EF calculations are not only correlated but also in high agreement. The corresponding Bland and Altman plot [Fig. 6(d)] confirms this result: the mean ± 2 SD of the differences in EFs computed from 2-D and 3-D images is $0.34\% \pm 5.4\%$. Thus, the SD of the differences of these two EF calculations is less than 3%.

The preliminary study carried out on healthy subjects showed high correlations and agreements between volume and EF computations from 2-D and reconstructed 3-D images. Even though care was taken to measure volumes accurately in both methods, the models used to estimate the LV volumes are rough, both in 2-D and in 3-D. Although particularly suited for normal LV measurements, they are of limited value for pathologic hearts. Moreover, quantitative measurements of the spatial accuracy of the reconstructions are needed to complete the qualitative assessments done by physicians. Additional clinical validations will be carried out to achieve the comparisons of both methods. Reconstructed 3-D images are expected to provide more accurate volume estimations than 2-D images in pathologic cases.

IV. CONCLUSIONS

The study presented in this correspondence shows that fast-rotating probes are available for cardiologists to per-

TABLE I

COMPARISON OF END-DIASTOLIC (V_D) AND END-SYSTOLIC (V_S) VOLUMES AND EJECTION FRACTION (EF) ESTIMATED BY TWO OPERATORS ON 3-D ECHOCARDIOGRAPHIC IMAGES OBTAINED FROM A DYNAMIC PHANTOM.

Parameters	Phantom values	Operator 1		Operator 2		Interoperator difference	
		Mean	SD	Mean	SD	Mean	SD
V_D (mL)	120	123.4	8.3	111.4	5.7	12.0	8.4
V_S (mL)	50	48.7	3.6	47	2.2	4.2	2.1
EF	0.58	0.60	0.03	0.58	0.02	0.03	0.02

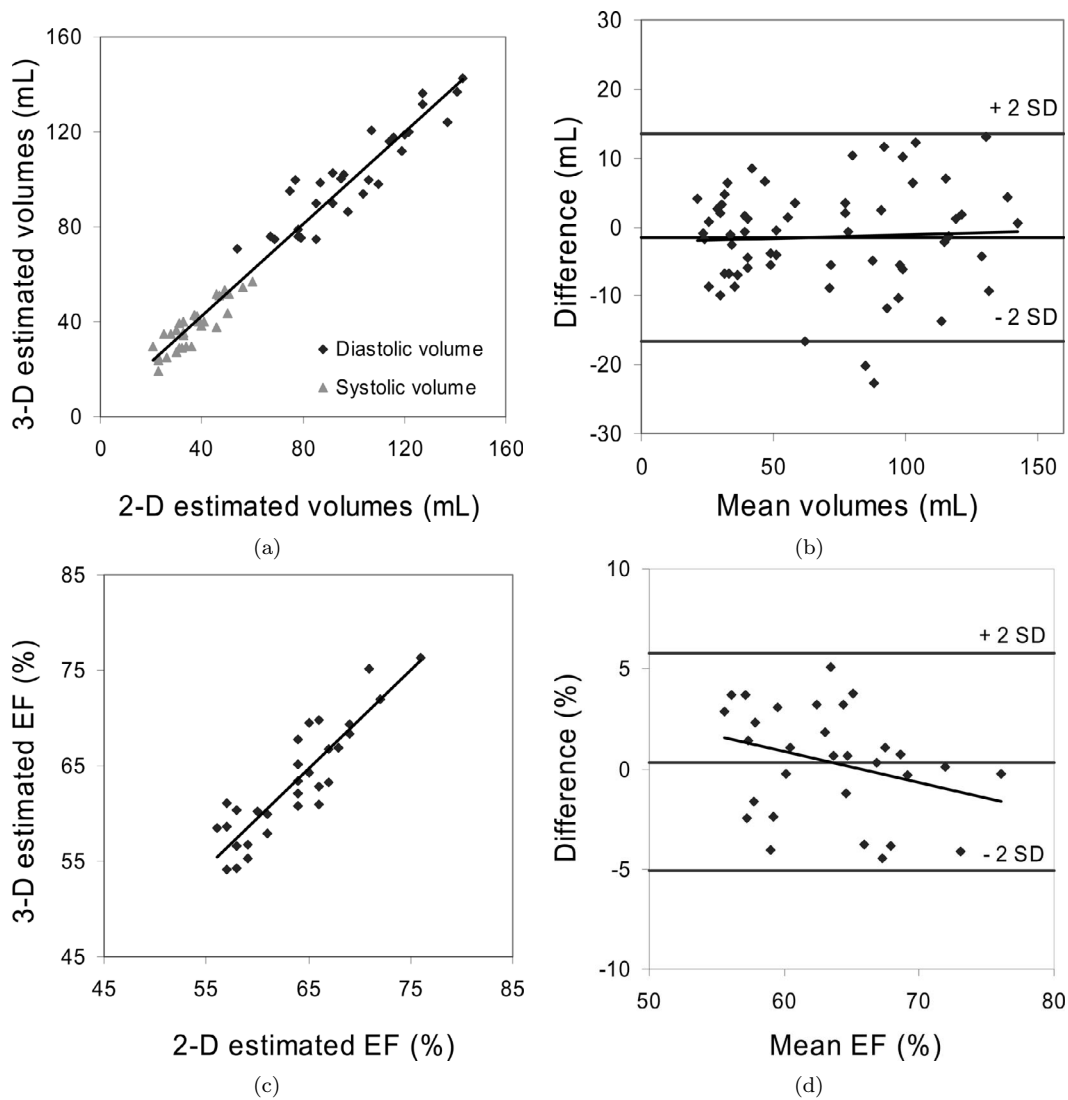


Fig. 6. Validation of the 3-D reconstructions. (a) Comparison of the volumes estimated with 2-D echocardiographic images and the 3-D reconstructed images. (b) Bland-Altman plots comparing differences in volume estimation from 2-D and 3-D echocardiography. (c) Comparison of the LV ejection fraction estimated with 2-D echocardiographic images and the 3-D reconstructed images. (d) Bland-Altman plots comparing EF estimation from 2-D echocardiographic images and the 3-D reconstructed images.

form 3-D echocardiography with data acquired during a single cardiac cycle. A dynamic cardiac phantom was used to quantify the variability of measurements. Then a clinical trial showed that LV volumes measured within reconstructed 3-D images are in agreement with volumes estimated on 2-D images using the classical Simpson method. Compared to RT3D probes that require specific equipment, rotating 2-D probes can be connected to standard ultrasound systems. Thus, they provide an easy and cheap way to introduce 3-D echocardiography within cardiology departments.

ACKNOWLEDGMENT

The authors wish to thank the Philips Ultrasound Company (loan of an HDI 5000 cardiac ultrasound system) and the Amsterdam Academic Medical Centre (rent of the dynamic cardiac phantom) for their interest and involvement in this study.

REFERENCES

- [1] A. Fenster and D. Downey, "3D ultrasound imaging: A review," *IEEE Eng. Med. Biol. Mag.*, vol. 15, no. 6, pp. 41–51, 1996.
- [2] M. Matsumoto, M. Inoue, S. Tamura, K. Tanaka, and H. Abe, "Three-dimensional echocardiography for spatial visualisation and volume calculation of cardiac structures," *J. Clin. Ultrasound*, vol. 9, no. 4, pp. 157–165, 1981.
- [3] G. R. Lockwood, J. R. Talman, and S. S. Brunke, "Real-time 3D ultrasound imaging using sparse synthetic aperture beamforming," *IEEE Trans. Ultrason., Ferroelect., Freq. Contr.*, vol. 45, no. 6, pp. 980–988, 1998.
- [4] R. Martin, G. Bashein, P. Detmer, and W. Moritz, "Ventricular volume measurement from a multiplanar transesophageal ultrasonic imaging system: An in vitro study," *IEEE Trans. Biomed. Eng.*, vol. 37, no. 5, pp. 442–449, 1990.
- [5] X. Ye, J. A. Noble, and D. Atkinson, "3-D freehand echocardiography for automatic left ventricle reconstruction and analysis based on multiple acoustic windows," *IEEE Trans. Med. Imag.*, vol. 21, no. 9, pp. 1051–1058, 2002.
- [6] G. I. Sanchez-Ortiz, G. J. T. Wright, N. Clarke, J. Declerck, A. P. Banning, and J. A. Noble, "Automated 3-D echocardiography analysis compared with manual delineations and SPECT MUGA," *IEEE Trans. Med. Imag.*, vol. 21, no. 9, pp. 1069–1076, 2002.
- [7] T. Nelson and D. Pretorius, "3D ultrasound image quality improvement using spatial compounding and 3D filtering," *Med. Phys.*, vol. 21, no. 6, pp. 998–999, 1994.
- [8] O. Gérard, A. C. Billon, J. M. Rouet, M. Jacob, M. Fradkin, and C. Allouche, "Efficient model-based quantification of left ventricular function in 3-D echocardiography," *IEEE Trans. Med. Imag.*, vol. 21, no. 9, pp. 1059–1068, 2002.
- [9] J. T. Yen and S. W. Smith, "Real-time rectilinear volumetric imaging," *IEEE Trans. Ultrason., Ferroelect., Freq. Contr.*, vol. 49, no. 1, pp. 114–124, 2002.
- [10] E. D. Angelini, A. F. Laine, S. Takuma, J. W. Holmes, and S. Homma, "LV volume quantification via spatiotemporal analysis of real-time 3-D echocardiography," *IEEE Trans. Med. Imag.*, vol. 20, no. 6, pp. 457–469, 2001.
- [11] C. Bonciu, R. Weber, and C. Léger, "4D reconstruction of the left ventricle during a single heart beat from ultrasound imaging," *Image Vision Comput.*, vol. 19, pp. 401–412, 2001.
- [12] R. Canals, G. Lamarque, and P. Chatain, "Volumetric ultrasound system for left ventricle motion imaging," *IEEE Trans. Ultrason., Ferroelect., Freq. Contr.*, vol. 46, no. 6, pp. 1527–1538, Nov. 1999.
- [13] A. Fitzgibbon, M. Pilu, and R. B. Fisher, "Direct least square fitting of ellipses," *IEEE Trans. Pattern Anal. Machine Intell.*, vol. 21, no. 5, pp. 476–480, May 1999.
- [14] J. J. N. Visser, E. Busemann-Sokole, H. van de Stadt, M. C. Shehata, J. Jaspers, W. Scheurs, S. P. Anroedh, and B. van Eck-Smit, "A new 3-D gated dynamic cardiac phantom: Quality control of volume and ejection fraction in gated myocardial SPECT.," presented at Fifth International Conference of Nuclear Cardiology, Vienna, Austria, May 2–5, 2001.